Published in final edited form as:
Nano Lett. 2009 June ; 9(6): 2354–2359. doi:10.1021/nl900872r.

Tissue- and Organ-Selective Biodistribution of NIR Fluorescent Quantum Dots

Hak Soo Choi[1], **Binil Itty Ipe**[2], **Preeti Misra**[1], **Jeong Heon Lee**[1], **Moungi G. Bawendi**[2,*], and **John V. Frangioni**[1,3,*]

[1] Division of Hematology/Oncology, Department of Medicine, Beth Israel Deaconess Medical Center, Boston, MA 02215

[3] Department of Radiology, Beth Israel Deaconess Medical Center, Boston, MA 02215

[2] Department of Chemistry, Massachusetts Institute of Technology, Cambridge, MA 02139

Abstract

A significant portion of the field of nanomedicine is predicated on being able to target nanoparticles to sites of disease. However, *in vivo* biodistribution and clearance of nanoparticles are poorly understood. In this study, a novel formulation of near-infrared fluorescent InAs(ZnS) quantum dots was synthesized and coated with a systematically increasing chain length of PEG. We found that varying PEG chain length resulted in major changes in organ/tissue-selective biodistribution and clearance from the body.

Keywords

Quantum dots; indium arsenide; near-infrared fluorescence; nanoparticles; PEGylation; biodistribution; clearance; *in vivo* imaging

The future success of nanoparticle-based nanomedicine requires nanoparticles of well-defined *in vivo* behavior. While significant progress has been made in the development of nanoparticles for both diagnostic and therapeutic applications (reviewed in [1,2]), there are still many unanswered questions regarding their biodistribution to sites of disease and their clearance, i.e., elimination from the body. The key determinants of biodistribution and clearance of nanoparticles are their chemical composition, hydrodynamic diameter (HD), shape, and surface charge.[3,4] The HD, in particular, has a profound effect on the biodistribution and clearance of nanoparticles, often in a non-linear fashion.[5–7]

Most studies in the field of nanotechnology focus on nanoparticles ranging from 10 to 100 nm in HD, which are poorly cleared from the body, if at all, and which eventually accumulate in the reticuloendothelial system (RES).[8–10] Although biocompatible polymers such as polyethylene glycol (PEG) have been used to increase solubility and prolong blood half-life, they only delay RES uptake due to the high molecular weights.[11–14] They also increase HD significantly, leading to increased background during imaging and diagnosis.[4,15] Nevertheless,

*Corresponding Authors: John V. Frangioni, M.D., Ph.D., Beth Israel Deaconess Medical Center, 330 Brookline Avenue, Room SL-B05, Boston, MA 02215, Phone: 617-667-0692 Fax: 617-667-0981, jfrangio@bidmc.harvard.edu, Moungi G. Bawendi, Ph.D., Massachusetts Institute of Technology, 77 Massachusetts Avenue, 6-221, Cambridge, MA 02139, Phone: 617-253-9796 Fax: 617-253-7030, mgb@mit.edu.

Supporting Information Available: Details of experimental methods, additional NIR fluorescence images, and a real-time *in vivo* imaging video. This material is available free of charge via the Internet at http://pubs.acs.org.

by introducing neutral and hydrophilic polymer chains, nanoparticles can avoid serum protein binding and can often achieve enhanced permeability and retention (EPR) in tumor model systems.[16–20]

Here we demonstrate controlled organ- and tissue-selective biodistribution and elimination routes of nanoparticles by varying the surface coating with different lengths of short chain PEGs, but without any specific targeting moieties. For this study, we prepared novel ultrasmall-sized near-infrared (NIR) fluorescent quantum dots (QDs) composed of an InAs core and a ZnS shell (Figure 1a and Supporting Information).[21] Transmission electronic microscopy (TEM, JEOL 200CX) was used to measure the inorganic core(shell) diameter, which averaged 3.2 nm (Figure 1b). Dihydrolipoic acid (DHLA) and DHLA conjugated to a systematically increasing chain length of PEG (DHLA-PEG, n = 2, 3, 4, 8, 14, 22) were prepared as solubilizing organic coatings to the ultrasmall NIR nanocrystals.[12,22] Gel-filtration chromatography (GFC) with simultaneous, full-spectrum (300 – 1000 nm) absorbance and fluorescence was used to characterize QDs with various coatings.[15] Final QDs dissolved in phosphate buffer at pH 7.4, ranged from 4.5 to 16 nm in HD as PEG repeating units varied from 0 to 22 (Figure 1c and Table 1). The typical full width at half maximum (FWHM) of the emission spectrum was 92 nm for the DHLA-PEGylated InAs(ZnS) QDs (Figure 1c and Supporting Information Figure S1). Quantum yields ranged from ≈10 to 20%, increasing with longer PEG length. For measurement of the effects of serum protein adsorption, 1 μM QDs were incubated in PBS, 100% rat serum, or 100% rat urine for 4 h at 37°C prior to loading 100 μL onto the GFC column. As shown in Figure 1c, the HDs of PEGylated QDs were stable in 100% rat serum and urine during 4 h incubation at 37°C, while DHLA-coated QDs bound serum proteins and increased their overall HD to >20 nm (data not shown).

The selection of organic coating for nanoparticles has profound effects on biodistribution and clearance *in vivo*. Specifically, the HD and surface charge of QDs are of paramount importance for their *in vivo* localization. Ideally, nanoparticles less than ≈5.5 nm HD with polar (non-ionic) or zwitterionic coatings can be readily excreted renally.[4,23] To synthesize such small QDs in the NIR, we have introduced various shells, such as ZnS, ZnSe, and ZnSeS, on InAs cores and have overcoated these core(shell) structures with mono- or bi-dentate thiolated ligands having different charges and lengths (Ipe et al., manuscript in preparation). However, it was extremely challenging to synthesize stable emissive NIR QDs having an HD ≤ 5.5 nm. We did, however, succeed in generating bright, ultrasmall NIR QDs with bidentate small ligands on InAs(ZnS) nanocrystals (Figure 1). Although a DHLA coating alone provided the smallest HD with InAs (ZnS) QDs (4.5 nm by GFC), these QDs were not stable in serum due to the propensity of the carboxylic acids of DHLA to bind serum proteins, which increased the final HD to over 20 nm. Adding neutral PEG units to DHLA permitted precise control of HD while maintaining stability of InAs(ZnS) QDs in serum and urine for over 4 h at 37°C (Figure 1).

To explore the effect of surface chemistry and HD on their behavior *in vivo*, the series of PEGylated NIR QDs were injected intravenously into Sprague-Dawley rats at a dose of 20 pmol/g animal weight, and their biodistribution and clearance were compared at 4 h post-injection using NIR fluorescence imaging (Figure 2). The NIR region of the electromagnetic spectrum (700 to 900 nm) is particularly important for this study because *in vivo* optical imaging requires high photon penetration into living tissue and low tissue autofluorescence.[24–26] For real-time live imaging, a custom intraoperative fluorescence imaging system was utilized.[27–29] For fluorescence excitation, 24 red LEDs (Marubeni Epitex, New York, NY) fitted with 667 ± 11 nm excitation filters (Chroma Technology, Brattleboro, VT) in custom holders were used. The emission filter used was a 720 nm long pass filter. As shown in Figure 2, QDs with a DHLA-PEG2 coating accumulated largely in the liver, whereas DHLA-PEG3 led QDs to the kidneys and bladder. QDs with DHLA-PEG4 coating had accelerated body excretion via the liver and kidneys. Interestingly, QDs with DHLA-PEG8, and to a lesser extent DHLA-PEG14,

accumulated in the pancreas (see video in online Supporting Information). QDs coated with DHLA-PEG14 were also excreted quickly through the liver to the intestine. QDs with DHLA-PEG22 (16 nm HD) exhibited poor clearance and were primarily found in the vasculature at 4 h post-injection.

To confirm the renal clearance of QDs, the kidneys were harvested 4 h post-injection and cross-sectional images were obtained (Figure 3 and Supporting Information Figure S2). DHLA-PEG4-coated NIR QDs (5.6 nm HD) passed through the glomerular filters resulting in high signal in the collecting system relative to the medulla and cortex. Despite their smaller size (5.1 nm HD), almost no QDs with DHLA-PEG2 coating were found in the kidneys, but rather were trapped by the liver. On the other hand, weak signals in the kidneys and bladder were seen with larger QDs over 6.5 nm HD (Supporting Information Figure S2). As mentioned above, DHLA-PEG8-coated QDs (6.5 nm HD), and to a lesser extent DHLA-PEG14-coated QDs (8.7 nm HD), accumulated in the pancreas. The largest QDs studied also accumulated in lymph nodes after intravenous injection.

After fluorescence imaging, animals were sacrificed and relevant tissues analyzed histologically to confirm QD localization (Figure 3, right two panels). For preparing frozen sections, major tissues and organs were resected 4 h post-injection, fixed in 10% formalin overnight, molded with OCT, and frozen in liquid nitrogen. Frozen sections were cut with 8 μm thickness and stained with hematoxylin and eosin (H&E, Histotec Laboratories). Liver, spleen, kidney, pancreas, intestine, muscle, and lymph nodes were examined by NIR fluorescence microscope. The excitation and emission filters used were 650 ± 22 nm and 710 ± 25 nm, respectively.

To perform quantitative assessment of biodistribution in blood, tissues, and organs, NIR QDs were labeled with ^{99m}Tc-MAS$_3$ by the addition of 80 μL of ^{99m}Tc-MAS$_3$-NHS (2 mCi) in DMSO to 1 mL of QDs (5 μM) in PBS, pH 7.8 supplemented with 1 mM cysteine. Blood clearance was measured by intermittent sampling of the tail vein. Increasing PEG chain length resulted in significantly enhanced blood retention time, delayed excretion through the renal and hepatic routes, and delayed tissue extravasation. DHLA-PEG4-coated QDs (5.6 nm HD) were found primarily in the bladder (47.0 ± 5.7 %ID), with distribution in the kidney (7.9 ± 3.8 %ID), liver (8.1 ± 5.6 %ID), and intestine (7.5 ± 4.2 %ID), likely representing QDs in the process of being excreted (Figure 4a, 4c). DHLA-PEG4-coated QDs appeared stable in urine from GFC analysis (Figure 4c). On the contrary, larger QDs (DHLA-PEG14; 8.7 nm HD) exhibited relatively high uptake in the liver (18.6 ± 2.6%) and intestine (21.4 ± 3.2%), and almost no signal in the kidneys and bladder (Figure 4b, 4c). The blood half-life ($t_{1/2\beta}$) of QDs (Figure 4c) with DHLA-PEG4 was over half that of QDs with DHLA-PEG14 (395 min vs. 922 min).

Usually, opsonized nanoparticles are recognized by macrophages, trapped in the RES (mainly liver and spleen), and degraded over a long time period.[30,31] PEGylation, presumably due to the hydrophilic character of the polymer chains,[32] greatly reduces trapping by the RES. Additionally, PEG chain length appears to play an important role in the biodistribution and clearance of nanoparticles. QDs coated with shorter PEG chain lengths (to maintain final HD ≤ 5.5 nm) should, in principle, be cleared by the kidneys. Indeed, DHLA-PEG3 (5.3 nm HD) and DHLA-PEG4 (5.6 nm HD) formulations appear to have the proper ratio of HD and hydrophilicity for rapid renal clearance. Interestingly, though, DHLA-PEG2-coating (4.5 nm HD) induced rapid trapping of QDs in liver, either due to specific chemical recognition of the short-chain PEG or increased relative hydrophobicity. DHLA-PEG8 provided adequate solubility in serum, but its size (6.5 nm HD) is above the threshold for renal excretion.[4] Instead, this formulation led to rapid excretion through the liver and into bile, and surprisingly, preferential accumulation in the parenchyma of the pancreas. The pancreas is an important

organ with very few known molecular targets, so the accumulation of specific PEG chain lengths is an unusual finding, and one that may lay the foundation for developing more specific targeting agents to the pancreas. Long PEG chain length increased QD blood half-life significantly, and rendered QDs more likely subject to hepatic clearance and uptake in lymph nodes. However, DHLA-PEG22-coated QDs (16 nm HD), were not excreted even by the liver after 4 h, and remained largely in the vasculature.

In this study, we have explored the effects of surface coating, HD, charge, and polarity on the biodistribution and clearance of emissive PEGylated NIR InAs(ZnS) QDs. Although PEG is typically considered an inert molecule, our study suggests that chain length, and thus chemical structure, has a major impact on the biodistribution and clearance of these nanoparticles. Increasing PEG chain length from 2 to 22 units not only resulted in predictable changes in HD, but also resulted in unpredictable targeting to the liver, kidney, pancreas, and lymph nodes. Ultra-short PEG chains (i.e., $n = 2$) retain a hydrophobic character and result in rapid uptake in liver, relatively long PEG chains (i.e., $n \geq 22$) are highly hydrophilic and remain in the vasculature for long periods of time, and intermediate chain lengths exhibit specific tissue and organ distribution and clearance.

Supplementary Material

Refer to Web version on PubMed Central for supplementary material.

Acknowledgments

The Biophysical Instrumentation Facility for the Study of Complex Macromolecular Systems (NSF-0070319 and NIH GM68762) is gratefully acknowledged. This work was supported in part by NIH grant #R33-EB-000673 (JVF and MGB), NIH grant #R01-CA-115296 (JVF), and a fellowship from the Charles A. King Trust, Bank of America, Co-Trustee (HSC). MGB also acknowledges support from the NIH funded MIT-Harvard NanoMedical Consortium (1U54-CA-119349, a Center of Cancer Nanotechnology Excellence). We thank Barbara L. Clough for editing and Eugenia Trabucchi for administrative assistance.

References

1. Nie S, Xing Y, Kim GJ, Simons JW. Annu Rev Biomed Eng 2007;9:257–88. [PubMed: 17439359]
2. Jin S, Ye K. Biotechnol Prog 2007;23:32–41. [PubMed: 17269667]
3. Alexis F, Pridgen E, Molnar LK, Farokhzad OC. Mol Pharm 2008;5:505–15. [PubMed: 18672949]
4. Choi HS, Liu W, Misra P, Tanaka E, Zimmer JP, Itty Ipe B, Bawendi MG, Frangioni JV. Nat Biotechnol 2007;25:1165–70. [PubMed: 17891134]
5. Khan MK, Nigavekar SS, Minc LD, Kariapper MS, Nair BM, Lesniak WG, Balogh LP. Technol Cancer Res Treat 2005;4:603–13. [PubMed: 16292880]
6. Balogh L, Nigavekar SS, Nair BM, Lesniak W, Zhang C, Sung LY, Kariapper MS, El-Jawahri A, Llanes M, Bolton B, Mamou F, Tan W, Hutson A, Minc L, Khan MK. Nanomedicine 2007;3:281–96. [PubMed: 17962085]
7. Frangioni JV. J Clin Oncol 2008;26:4012–21. [PubMed: 18711192]
8. Ballou B, Ernst LA, Andreko S, Harper T, Fitzpatrick JA, Waggoner AS, Bruchez MP. Bioconjug Chem 2007;18:389–96. [PubMed: 17263568]
9. Ballou B. Curr Top Dev Biol 2005;70:103–20. [PubMed: 16338339]
10. Zhang L, Gu FX, Chan JM, Wang AZ, Langer RS, Farokhzad OC. Clin Pharmacol Ther 2008;83:761–9. [PubMed: 17957183]
11. Ballou B, Lagerholm BC, Ernst LA, Bruchez MP, Waggoner AS. Bioconjug Chem 2004;15:79–86. [PubMed: 14733586]
12. Uyeda HT, Medintz IL, Jaiswal JK, Simon SM, Mattoussi H. J Am Chem Soc 2005;127:3870–8. [PubMed: 15771523]

13. Chen X, Park R, Shahinian AH, Bading JR, Conti PS. Nucl Med Biol 2004;31:11–9. [PubMed: 14741566]
14. Dixit V, Van den Bossche J, Sherman DM, Thompson DH, Andres RP. Bioconjug Chem 2006;17:603–9. [PubMed: 16704197]
15. Frangioni JV, Kim SW, Ohnishi S, Kim S, Bawendi MG. Methods Mol Biol 2007;374:147–60. [PubMed: 17237537]
16. Moghimi SM, Porter CJ, Muir IS, Illum L, Davis SS. Biochem Biophys Res Commun 1991;177:861–6. [PubMed: 2049107]
17. Cai W, Shin DW, Chen K, Gheysens O, Cao Q, Wang SX, Gambhir SS, Chen X. Nano Lett 2006;6:669–76. [PubMed: 16608262]
18. Schipper ML, Cheng Z, Lee SW, Bentolila LA, Iyer G, Rao J, Chen X, Wu AM, Weiss S, Gambhir SS. J Nucl Med 2007;48:1511–8. [PubMed: 17704240]
19. Duncan R. Nat Rev Cancer 2006;6:688–701. [PubMed: 16900224]
20. Yuan TL, Choi HS, Matsui A, Benes C, Lifshits E, Luo J, Frangioni JV, Cantley LC. Proc Natl Acad Sci U S A 2008;105:9739–44. [PubMed: 18621722]
21. Zimmer JP, Kim SW, Ohnishi S, Tanaka E, Frangioni JV, Bawendi MG. J Am Chem Soc 2006;128:2526–7. [PubMed: 16492023]
22. Mattoussi H, Mauro JM, Goldman ER, Anderson GP, Sundar VC, Mikulec FV, Bawendi MG. J Am Chem Soc 2000;122:12142–50.
23. Liu W, Choi HS, Zimmer JP, Tanaka E, Frangioni JV, Bawendi M. J Am Chem Soc 2007;129:14530–1. [PubMed: 17983223]
24. Frangioni JV. Curr Opin Chem Biol 2003;7:626–34. [PubMed: 14580568]
25. Kobayashi H, Hama Y, Koyama Y, Barrett T, Regino CA, Urano Y, Choyke PL. Nano Lett 2007;7:1711–6. [PubMed: 17530812]
26. Hama Y, Koyama Y, Urano Y, Choyke PL, Kobayashi H. J Invest Dermatol 2007;127:2351–6. [PubMed: 17522707]
27. Kim S, Lim YT, Soltesz EG, De Grand AM, Lee J, Nakayama A, Parker JA, Mihaljevic T, Laurence RG, Dor DM, Cohn LH, Bawendi MG, Frangioni JV. Nat Biotechnol 2004;22:93–7. [PubMed: 14661026]
28. Tanaka E, Choi HS, Fujii H, Bawendi MG, Frangioni JV. Ann Surg Oncol 2006;13:1671–81. [PubMed: 17009138]
29. Tanaka E, Choi HS, Humblet V, Ohnishi S, Laurence RG, Frangioni JV. Surgery 2008;144:39–48. [PubMed: 18571583]
30. Minchin R. Nat Nanotechnol 2008;3:12–3. [PubMed: 18654442]
31. Dobrovolskaia MA, McNeil SE. Nat Nanotechnol 2007;2:469–78. [PubMed: 18654343]
32. Brannon-Peppas L, Blanchette JO. Adv Drug Deliv Rev 2004;56:1649–59. [PubMed: 15350294]

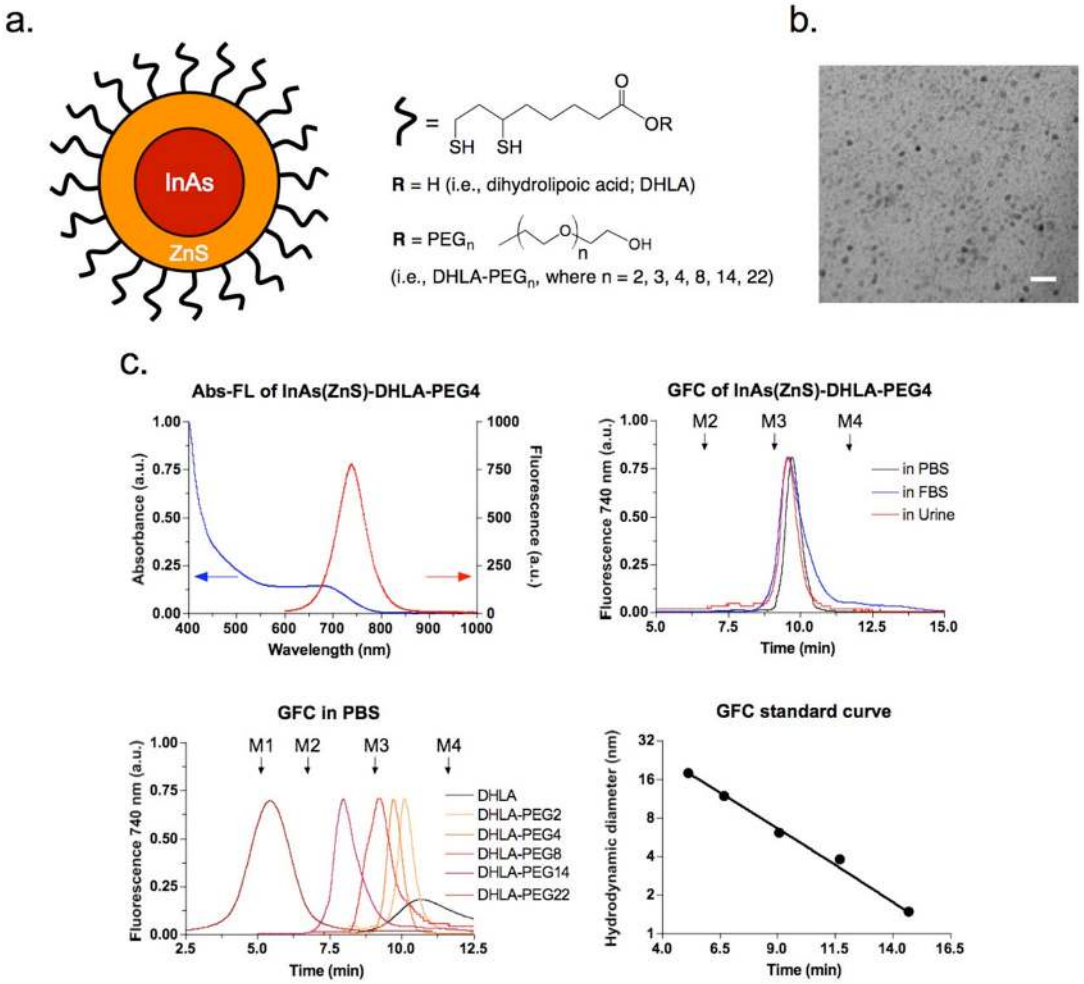

Figure 1.

Structural and optical properties of PEGylated NIR QDs: (a) InAs(ZnS) QDs with systematically increasing PEG chain length attached through a DHLA linker. (b) TEM of InAs (ZnS)-DHLA-PEG4 (core + shell = 3.2 nm). Scale bar = 10 nm. (c) Representative absorbance and fluorescence emission (λ_{Exc} = 532 nm) spectra of PEGylated NIR QDs (top left). Stability of PEGylated NIR QDs in PBS, FBS, and urine after 4 h incubation at 37°C (top right). GFC (mobile phase = PBS, pH 7.4) analysis of PEGylated InAs(ZnS) QDs (bottom left). Molecular weight markers M1 (thyroglobulin; 669 kDa, 18.8 nm HD), M2 (γ-globulin; 158 kDa, 11.9 nm HD), M3 (ovalbumin; 44 kDa, 6.13 nm HD), and M4 (myoglobin; 17 kDa, 3.83 nm HD) are shown by arrows. GFC standard curve (bottom right).

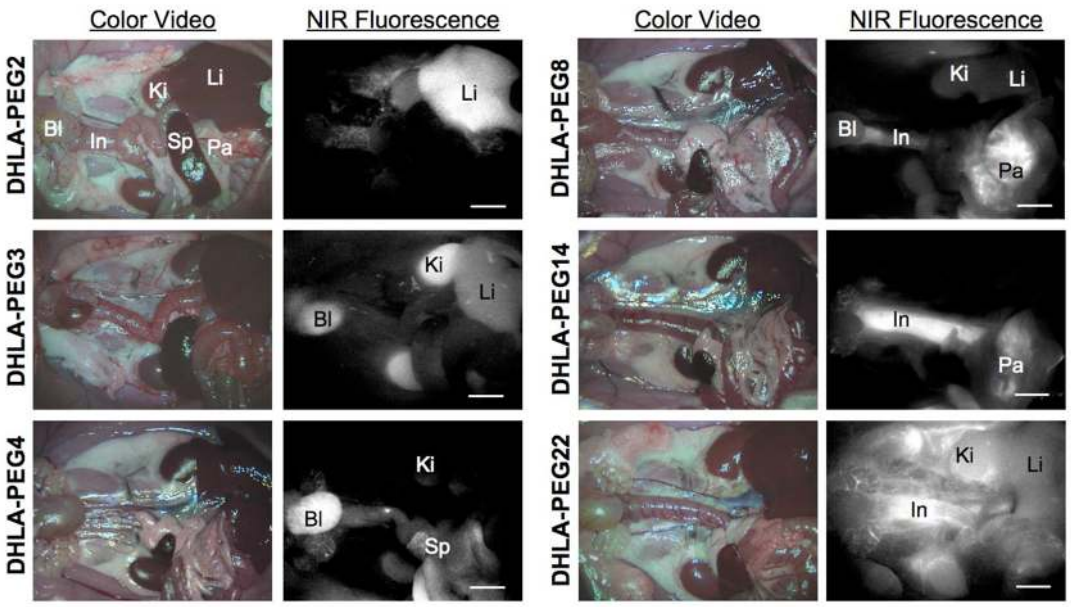

Figure 2.

In vivo NIR fluorescence imaging of NIR QDs in Sprague-Dawley rats 4 h post-injection. Shown are InAs(ZnS) QDs coated with DHLA-PEG2, DHLA-PEG3, DHLA-PEG4, DHLA-PEG8, DHLA-PEG14, and DHLA-PEG22. Abbreviations used are: Ki, kidneys; Bl, bladder; Li, liver; Pa, pancreas; Sp, spleen; and In, intestine. Shown are representative images (from n = 3 separate animal experiments using 3 different lots of QDs) of color video (left) and NIR fluorescence (right). $\lambda_{Exc} = 667 \pm 11$ nm; $\lambda_{Em} = 720$ nm long pass. NIR fluorescence images have identical exposure times and normalizations. Scale bar = 500 μm.

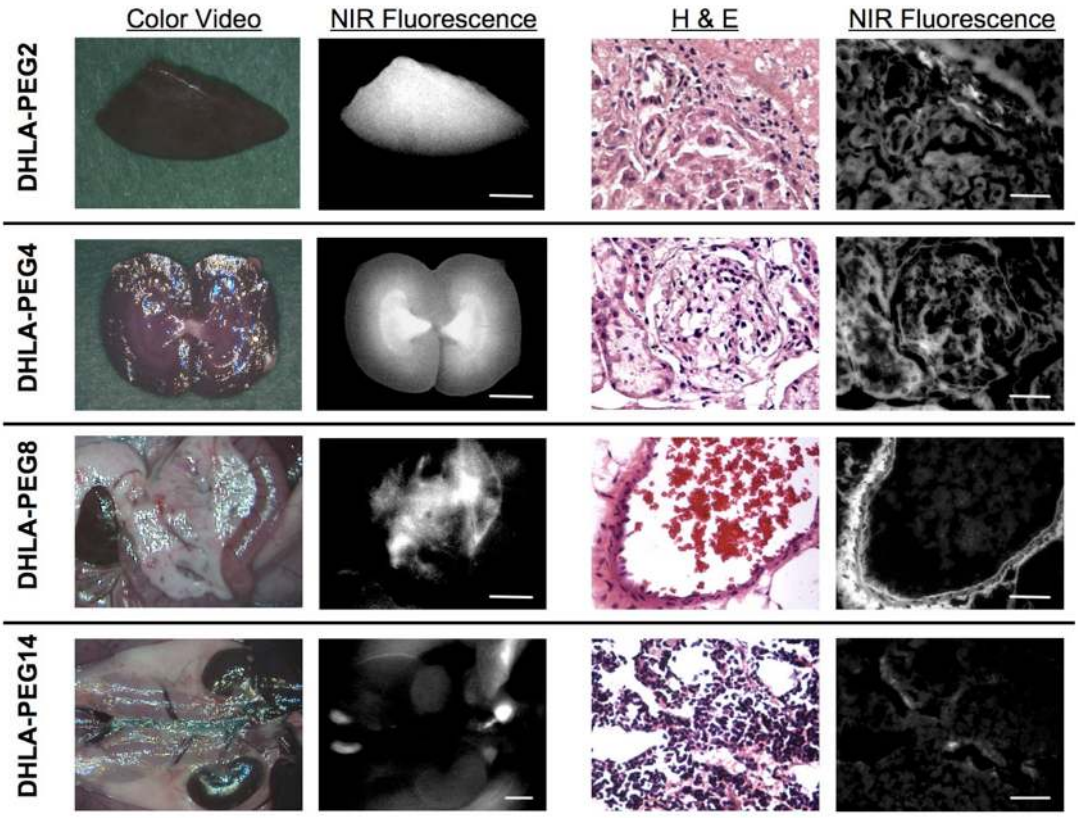

Figure 3.

Organ/tissue biodistribution of NIR QDs 4 h post-injection. From top to bottom are InAs(ZnS) NIR QDs coated with DHLA-PEG2 (liver), DHLA-PEG4 (kidney), DHLA-PEG8 (pancreas), and DHLA-PEG14 (lymph nodes). Shown are representative images (from n = 3 separate animal experiments using 3 different lots of QDs) of each organ/tissue by color video and NIR fluorescence (left two panels). Scale bar = 500 μm. Also shown are representative histological images from the same organ/tissue obtained during histological analysis of frozen sections (right two panels). NIR fluorescence images have identical exposure times and normalizations. Scale bar = 50 μm.

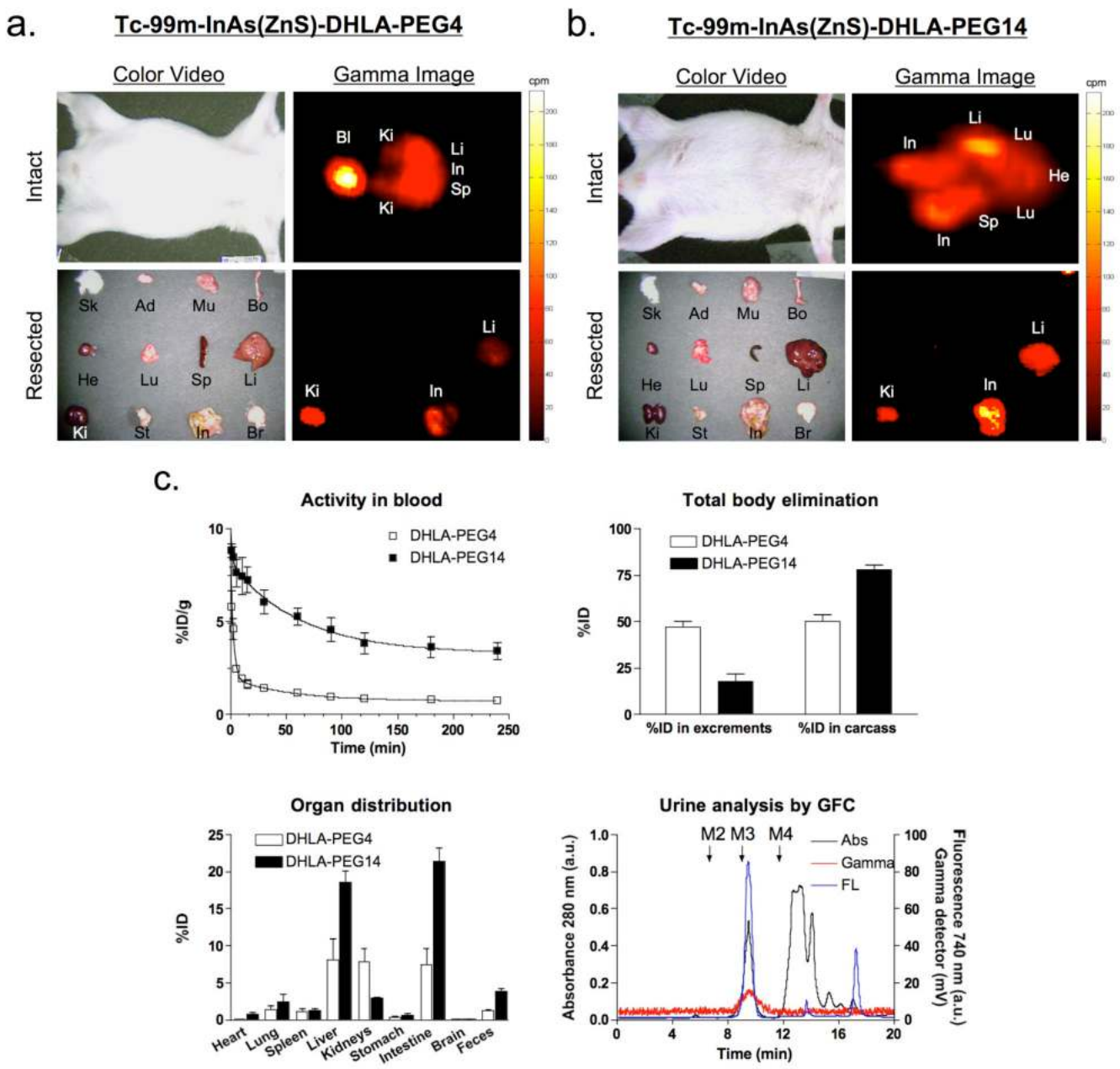

Figure 4.

Biodistribution and total body elimination of ^{99m}Tc-conjugated NIR QDs in CD-1 mice: Radioscintigraphic images of (a) ^{99m}Tc-InAs(ZnS)-DHLA-PEG4 (5.6 nm HD) and (b) ^{99m}Tc-InAs(ZnS)-DHLA-PEG14 (8.7 nm HD) 4 h post-intravenous injection. Shown are the color video (left) and Anger camera gamma-ray images (right) of intact animals immediately after sacrifice (top row), and of organs after resection (bottom row). Abbreviations used are: Sk, skin; Ad, adipose; Mu, muscle; Bo, bone; He, heart; Lu, lungs; Sp, spleen; Li, liver; Ki, kidneys; St, stomach; In, intestine; Br, brain; and Bl, bladder. (c) Blood concentration (%ID/g; top left), total body clearance (%ID; top right), and quantitative organ distribution (%ID; bottom left) of ^{99m}Tc-InAs(ZnS)-DHLA-PEG4 (white bar) and ^{99m}Tc-InAs(ZnS)-DHLA-PEG14 (black bar) after well counting. Each point represents the mean ± S.D. of n = 3 animals per QD lot. ^{99m}Tc-InAs(ZnS)-DHLA-PEG4 was identified intact in urine 4 h post-injection (bottom

right). Tracings include absorbance at 280 nm (solid black curve), fluorescence at 740 nm (solid blue curve), and gamma-ray detector (red curve).

Table 1

Organ-Selective Biodistribution of NIR QDs as a Function of Hydrodynamic Diameter

Ligand	HD[a] (nm)	Tissue									
		Ki	Bl	Li	Bi	Pa	Sp	Du	In	LN	Bd
DHLA	4.5	+	−	++	−	−	−	−	+	−	−
DHLA-PEG2	5.1	+	−	+++	−	−	−	+	+	−	−
DHLA-PEG3	5.3	+++	++	++	−	−	+	+	+	−	−
DHLA-PEG4	5.6	++	+++	+	−	+	++	+	++	+	+
DHLA-PEG8	6.5	−	++	+	−	+++	−	+	++	++	+
DHLA-PEG14	8.7	−	−	+	−	++	−	++	+++	+++	++
DHLA-PEG22	16.0	−	−	+	−	+	−	++	++	+++	+++

[a]HD was calculated by the following equation in Prism (an exponential decay equation): HD = A*exp(−B*X). Where: A = 64.92; B = 0.253; R^2 = 0.989. Abbreviations used are: Ki, kidneys; Bl, bladder; Li, liver; Bi, bile ducts; Pa, pancreas; Sp, spleen; Du, duodenum; In, intestine; LN, lymph nodes; and Bd, blood. Each point represents the mean ± S.D. of N = 5 animals. The signal-to-background ratio (SBR) of each organ relative to the abdominal wall was quantified and labeled as −; ≤ 1, +; 1 to 2, ++; 2 to 3, and +++; > 3.